Low-Discrepancy Blue Noise Sampling
Supplementary Material

Abdalla G. M. Ahmed[1] Hélène Perrier [2] David Coeurjolly[2] Victor Ostromoukhov[2]
Jianwei Guo[3] Dong-Ming Yan[3] Hui Huang [4,5] Oliver Deussen[1,5]

[1]University of Konstanz [2]Université de Lyon
[3]NLPR, Institute of Automation, CAS [4]Shenzhen University [5]SIAT

This supplementary material contains various results of the LDBN Sampler. In Section 1 we detail the impact of the optimization table's parameters on the final sampling, whereas in Section 2 we compare the results produced by our sampler with those produced by several state-of-the-art methods.

1 Influence of the optimization parameters

Our sampler relies on an optimization table, containing lists of permutations on chunks of a target set. In this section we present how the parameters m (the size of the permutation chunks) and t (the size of the target set) impact the resulting point set.

As t gets smaller with respect to the generated set, the replication process leads to worse results due to replication. This is illustrated Figure 4. On the other hand, as t increases, the memory footprint of the table increases. We found $t = 128$ to be a good tradeoff.

The m parameter controls how well the output of LDBN will match the given target pointset, Figure 2, and the target spectrum, Figure 1. However, if m increases too much, the discrepancy will degrade, as shown in Figure 3. Figure 2 illustrates how m impacts the matching of samples. Empirically, $m = 16$ appears as a good setting.

Figure 1 presents the Fourier spectra obtained with the LDBN sampler, for different values of m and t.

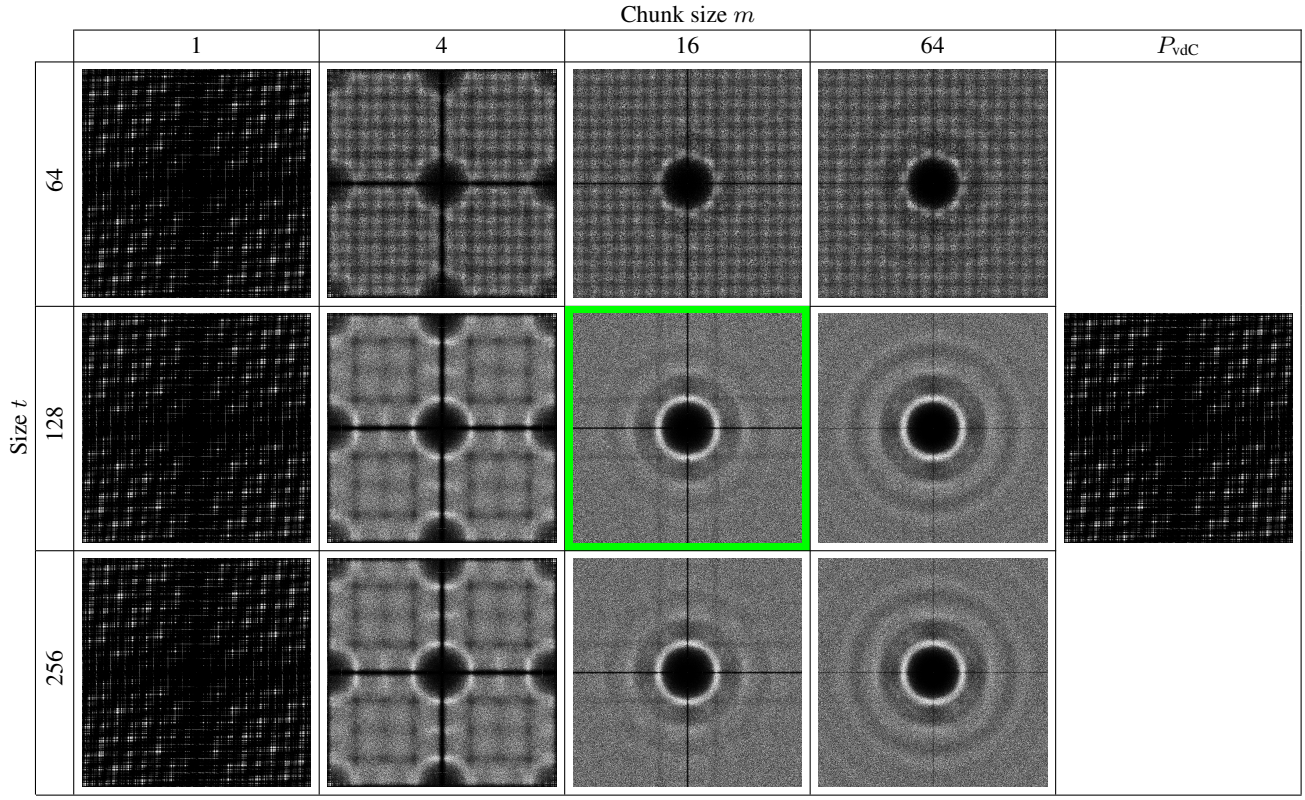

Figure 1: *Fourier spectra from pointsets with 16K samples, obtained using our method with different table size. As can be seen, the bigger the chunks m, the more Blue Noise the spectra, but if m increases too much, the Low Discrepancy property degrades. Also, as we increase t, we need less and less replication to generate our point sets which leads to cleaner spectra but at the cost of an increase in the memory requirements. In our tests, the parameters $m = 16$ and $t = 128$ are a good tradeoff. If you can't see those results due to a filtering or scaling from your pdf viewer, you may find on the project website a html bundle presenting the same results without scaling or filtering.*

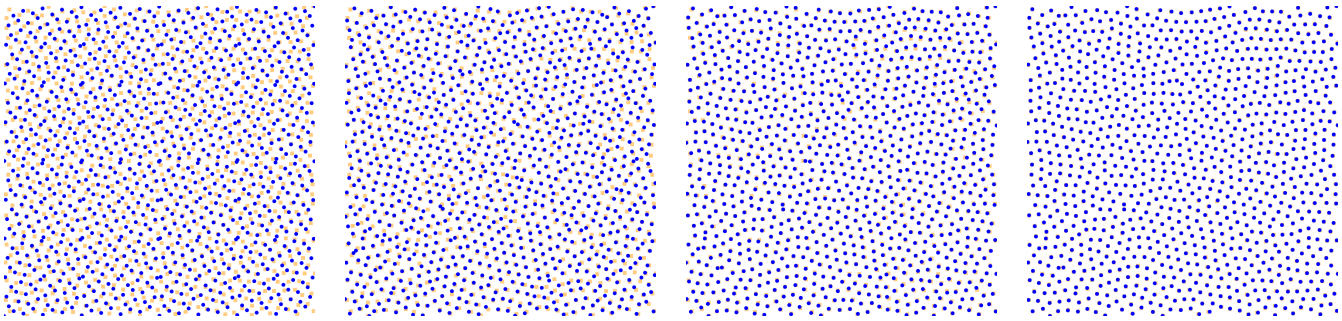

(a) *m=1* **(b)** *m=4* **(c)** ***m=16*** **(d)** *m=64*

Figure 2: *Error in approximating a target set (orange squares) by rearranging our P_{vdC} LD template (blue circles); using different values of the permutation chunk size m. At $m = 16$ the result is already close to the target. Stepping further would degrade the discrepancy (Figure 3), but more important, it means a 100% increase in the memory footprint, since a pair of permutations in $\{0...15\}$ can be stored in a single byte. It is far better investing the table size in increasing t than in producing closer approximation of an inherently stochastic target. Thus, from this perspective we choose m to be 16.*

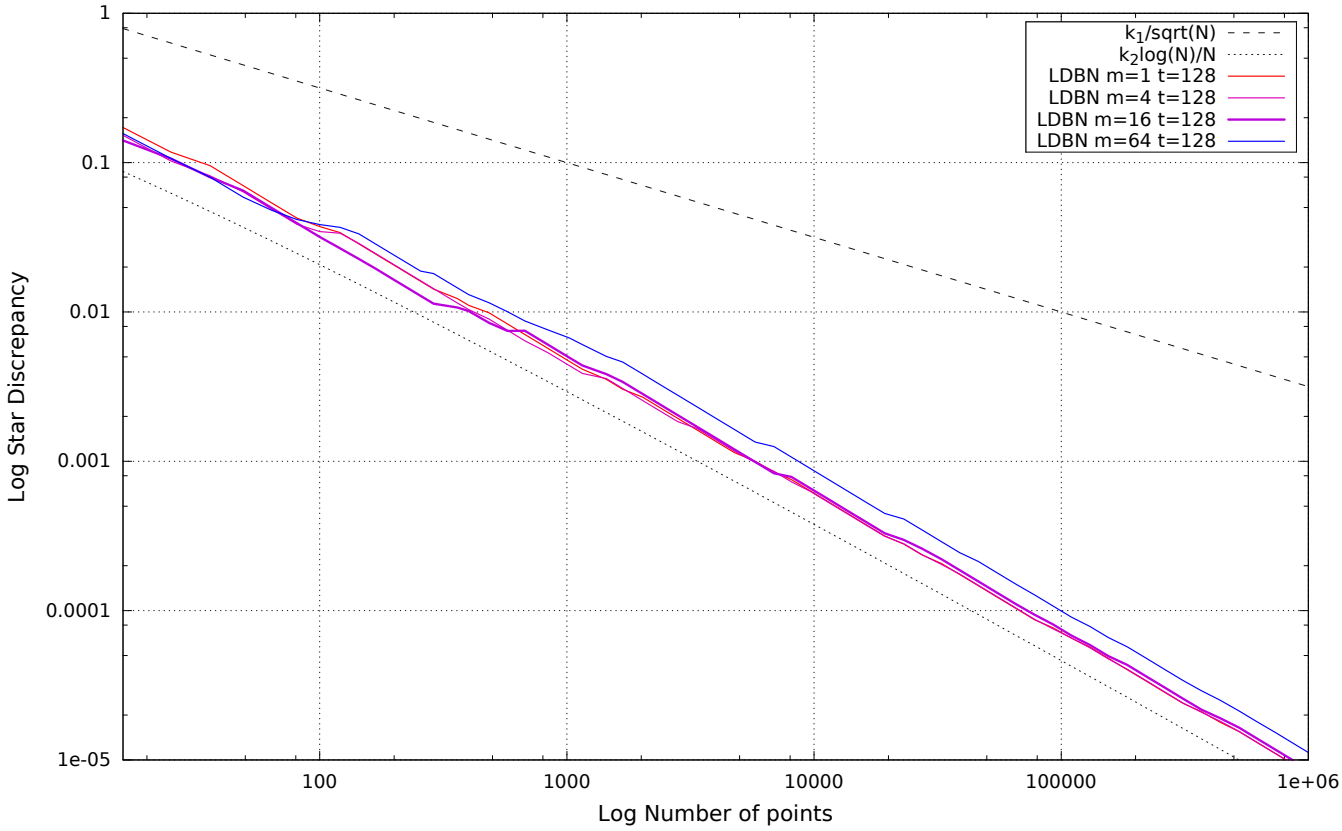

Figure 3: *Discrepancy of LDBN as the chunk size m increases for $t = 128$. Note that if $m \geq 64$, the discrepancy degrades.*

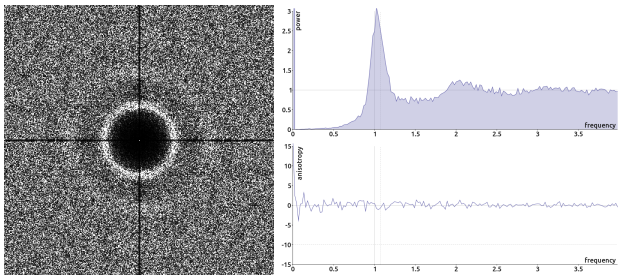

(a) *2025*

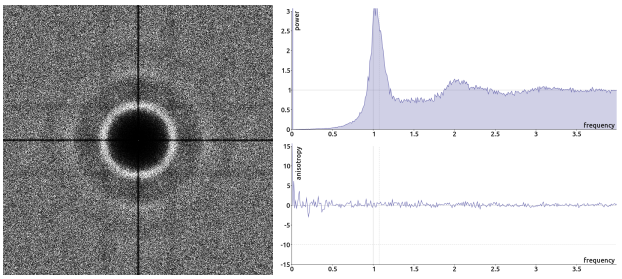

(b) *8100*

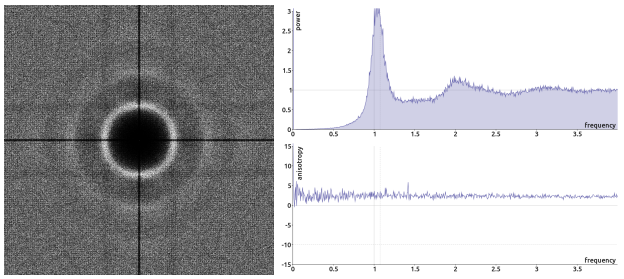

(c) *31684*

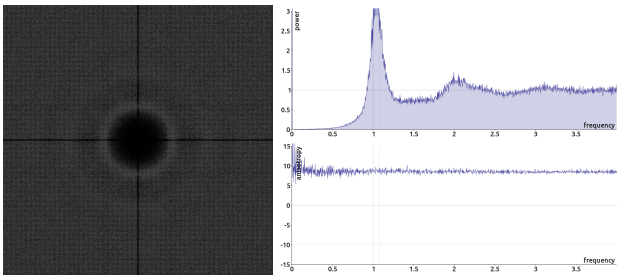

(d) *65536*

Figure 4: *Evolution of the spectra of our sampler when increasing the number of samples with* $m = 16$ *and* $t = 128$.

Ours

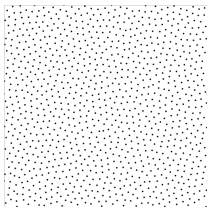

(a) *LDBN with Blue Noise target*

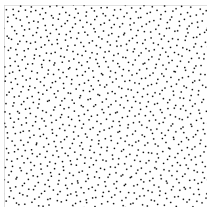

(b) *LDBN with Step target*

Blue Noise

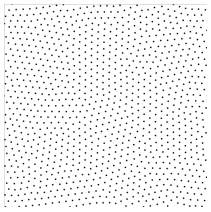

(c) *CVT [Lloyd 1982]*

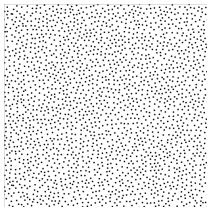

(d) *Wang Tiles [Kopf et al. 2006]*

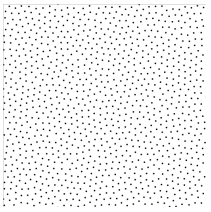

(e) *FPO [Schlömer et al. 2011]*

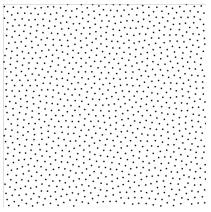

(f) *BNOT [de Goes et al. 2012]*

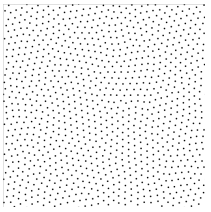

(g) *CapCVT [Chen et al. 2012]*

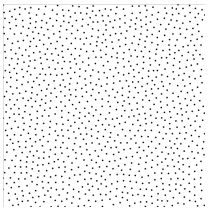

(h) *Polyhexes [Wachtel et al. 2014]*

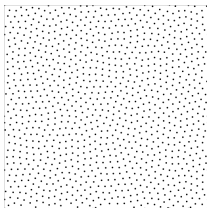

(i) *AA Patterns [Ahmed et al. 2015]*

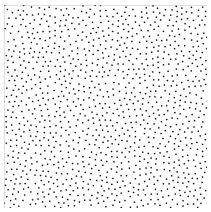

(j) *Poisson*

Low-Discrepancy

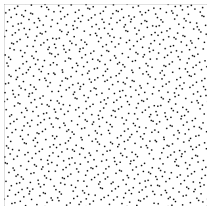

(k) *Halton [Halton 1960]*

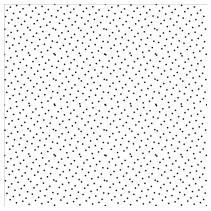

(l) *Hammersley [Hammersley 1960]*

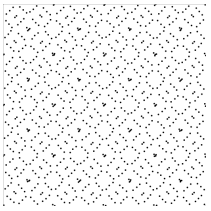

(m) *Sobol [Sobol' 1967]*

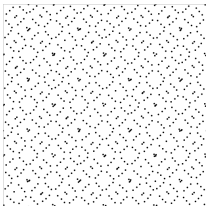

(n) *Faure [Faure 1982]*

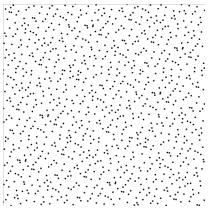

(o) *Niederreiter [Niederreiter 1988]*

Other

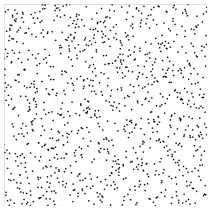

(p) *NRooks [Shirley 1991]*

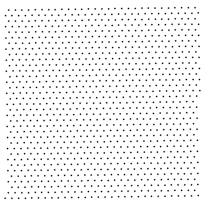

(q) *Rank1 [Keller 2004]*

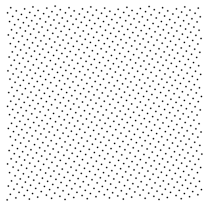

(r) *Rank1Fibo [Keller 2004]*

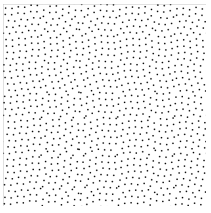

(s) *CMJ [Kensler 2013]*

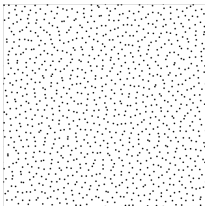

(t) *Step [Heck et al. 2013]*

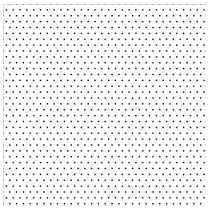

(u) *HexagonalGrid*

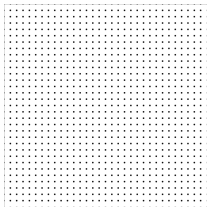

(v) *RegularGrid*

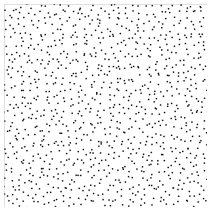

(w) *Stratified*

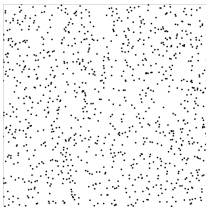

(x) *Whitenoise*

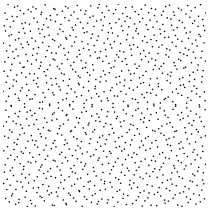

(y) *Owen's Scrambling [Kollig and Keller 2002]*

Figure 5: *Pointset distributions of our method and all the methods we compare ourselves to with 1024 points. Note that the root tile for Wang Tiles contains 2048 samples, therefore the pointsets cannot contain less than 2048 samples. The methods are organized between the Blue Noise methods, the Low Discrepancy methods, and the other methods (that are neither Blue Noise nor Low Discrepancy).*

2 Additional experiments

In this section, we present a comparison of several samplers (illustrated Figure 5). For simplicity and visualization clarity, we grouped them into three categories, the Blue Noise methods, the Low Discrepancy methods, and other methods. Those categories are detailed below. The settings for all experiments is detailed in the paper. We compare 4 characteristics of each sampler,

- the evolution of the star discrepancy of each sampler with a $(O)(n^2)$ algorithm
- the integration variance while integrating over both analytical scenes (disk, box arrangements) and HDR images
- the Fourier spectra
- the anti aliasing property is evaluated with the zoneplate test. This test reconstructs the function $\sin(x^2 + y^2)$ using a single sample per pixel and a Mitchell reconstruction filter.

2.1 Blue Noise methods

This category of methods generates samples with a Blue Noise spectrum. Blue Noise was defined by Ulichney in [Ulichney 1988] as

- Low frequency cut-off at principal frequency
- Sharp transition region
- Flat high frequency "Blue Noise" region

In Figure 8 you will see different spectra obtained by Blue Noise methods.

It can be seen that our method is the only one to present a black cross axis aligned. Therefore, none of the other methods are low discrepancy methods (as preventing point alignment in the projections is a mandatory condition for low discrepancy). This is further illustrated in Figure 10 where we compare the discrepancy of our method compared to Blue Noise ones.

Pointsets with a Blue Noise spectrum are known to have a good integration variance (convergence in $\mathcal{O}\left(\frac{1}{N\sqrt{N}}\right)$ [Pilleboue et al. 2015]). This is visible Figure 6 and Figure 6.

Furthermore, Blue Noise spectrum do not lead to any structured aliasing artefact. This is shown in Figure 9. We tested our samplers on the zoneplate aliasing test $\sin(x^2 + y^2)$ on the domain $[0, 1)$.

However, methods generating Blue Noise spectra usually present one of those two issues; they are either very slow to compute due to the iterative optimization done on the point set, or require precomputed tiles that are very memory consuming. Some methods exists that perform very fast Poisson Disk sampling [Dunbar and Humphreys 2006]. However, Poisson Disk point patterns lead to slower variance convergence rates than other Blue Noise samplers ([Pilleboue et al. 2015]).

Our sampler however, is very fast and has a very low memory footprint. Figure 6 and Figure 7 present the integration performances of Blue Noise methods compared to ours.

2.2 Low Discrepancy methods

This category of methods generates point sets or sequences with Low Discrepancy. Figure 15 presents the measured discrepancies for Low discrepancy samplers. We can see on this graph that, as was theoretically proven, our method has a similar discrepancy as the state of the art low discrepancy methods.

The major issue with low discrepancy samplers, is that their spectra usually present spurious peaks, as can be seen in Figure 13. It can be noted that the only method that does not present peaks is ours. This has a major consequence, since those peaks in the Fourier spectra converts into very disturbing aliasing artefacts.

Therefore our method is the only low discrepancy method that allows a correct reconstruction of the zoneplate aliasing test $sin(x^2 + y^2)$. This is illustrated in Figure 14.

In Figure 12 and Figure 11, we can see the integration convergence rate of Low Discrepancy samplers compared to our sampler.

Note the special case of Owen's scrambling. This scrambling is applied on a low discrepancy sampler to remove the peaks in its spectra. It should therefore be part of the Low Discrepancy section of this supplementary. However, since it's not a sampler itself but a scrambling over a sampler, we chose to move it to the next section. Rank1 is another Low Discrepancy sampler that was moved to the next section. Since it's closely related to the regular grid, we chose to have both of them in the same section to be able to compare directly between the two.

2.3 Other methods

Here, we compare our sampler with latinized and stratified samplers and other methods that are (for most of them) neither Blue Noise nor Low Discrepancy methods.

Latinized and stratified samplers usually maintain a lower discrepancy than the Blue Noise samplers because the inherent stratification reduces discrepancy and latinization can explicitly prevent that two points fall in the same place by projection.

Some of them also use randomization to try and prevent the peaks in the Fourier spectrum and therefore limit aliasing.

The main advantage of those methods is usually their simplicity in implementation and their speed. The associated drawback being that since most of them are not Blue Noise nor Low Discrepancy, they are often less efficient in practice than the methods presented in the last two sections. We can note the exception of Owen's scrambling that randomize a Low Discrepancy sampler to limit aliasing. However, even though it performs better than usual Low Discrepancy samplers, it is not as efficient as Blue Noise against aliasing.

We present the Fourier spectra of those various samplers in Figure 18, along with their discrepancy in Figure 20 and their variance in integration in Figure 16 and in Figure 17. We also demonstrate how they perform in the zoneplate aliasing test $sin(x^2 + y^2)$ in Figure 19.

References

AHMED, A. G. M., HUANG, H., AND DEUSSEN, O. 2015. AA patterns for point sets with controlled spectral properties. *ACM Trans. Graph. 34*, 6 (Oct.), 212:1–212:8.

CHEN, Z., YUAN, Z., CHOI, Y.-K., LIU, L., AND WANG, W. 2012. Variational blue noise sampling. *IEEE Transactions on Visualization and Computer Graphics 18*, 10 (Oct.), 1784–1796.

DE GOES, F., BREEDEN, K., OSTROMOUKHOV, V., AND DESBRUN, M. 2012. Blue noise through optimal transport. *ACM Trans. Graph. 31*, 6 (Nov.), 171:1–171:11.

DUNBAR, D., AND HUMPHREYS, G. 2006. A spatial data structure for fast poisson-disk sample generation. *ACM Trans. Graph. 25*, 3 (July), 503–508.

FAURE, H. 1982. Discrépances de suites associées à un système de numération (en dimension s). *Acta Arithmetica 41*, 4, 337–351.

HALTON, J. H. 1960. On the efficiency of certain quasi-random sequences of points in evaluating multi-dimensional integrals. *Numerische Mathematik 2*, 1, 84–90.

HAMMERSLEY, J. M. 1960. Monte Carlo methods for solving multivariable problems. *Annals of the New York Academy of Sciences 86*, 3, 844–874.

HECK, D., SCHLÖMER, T., AND DEUSSEN, O. 2013. Blue noise sampling with controlled aliasing. *ACM Trans. Graph. 32*, 3, 25:1–25:12.

KELLER, A. 2004. Stratification by rank-1 lattices. *Monte Carlo and Quasi-Monte Carlo Methods 2002*, 299–313.

KENSLER, A. 2013. Correlated multi-jittered sampling. *Pixar Technical Memo 13-01 7*, 86–112.

KOLLIG, T., AND KELLER, A. 2002. Efficient multidimensional sampling. In *Computer Graphics Forum*, vol. 21, Wiley Online Library, 557–563.

KOPF, J., COHEN-OR, D., DEUSSEN, O., AND LISCHINSKI, D. 2006. Recursive Wang tiles for real-time blue noise. *ACM Trans. Graph. 25*, 3, 509–518.

LLOYD, S. 1982. Least squares quantization in PCM. *IEEE Transactions on Information Theory 28*, 2, 129–137.

MITCHELL, D. P., AND NETRAVALI, A. N. 1988. Reconstruction filters in computer-graphics. In *ACM Siggraph Computer Graphics*, vol. 22, ACM, 221–228.

NIEDERREITER, H. 1988. Low-discrepancy and low-dispersion sequences. *Journal of Number Theory 30*, 1 (sep), 51–70.

PILLEBOUE, A., SINGH, G., COEURJOLLY, D., KAZHDAN, M., AND OSTROMOUKHOV, V. 2015. Variance analysis for Monte Carlo integration. *ACM Trans. Graph. (Proc. SIGGRAPH) 34*, 4, 124:1–124:14.

SCHLÖMER, T., HECK, D., AND DEUSSEN, O. 2011. Farthest-point optimized point sets with maximized minimum distance. In *Symp. on High Performance Graphics*, 135–142.

SHIRLEY, P. 1991. Discrepancy as a quality measure for sample distributions. In *Proc. Eurographics '91*, 183–194.

SOBOL', I. M. 1967. On the distribution of points in a cube and the approximate evaluation of integrals. *Zhurnal Vychislitel'noi Matematiki i Matematicheskoi Fiziki 7*, 4, 784–802.

ULICHNEY, R. 1988. Dithering with blue noise. *Proceedings of the IEEE 76*, 1 (Jan), 56–79.

WACHTEL, F., PILLEBOUE, A., COEURJOLLY, D., BREEDEN, K., SINGH, G., CATHELIN, G., DE GOES, F., DESBRUN, M., AND OSTROMOUKHOV, V. 2014. Fast tile-based adaptive sampling with user-specified Fourier spectra. *ACM Trans. Graph. 33*, 4.

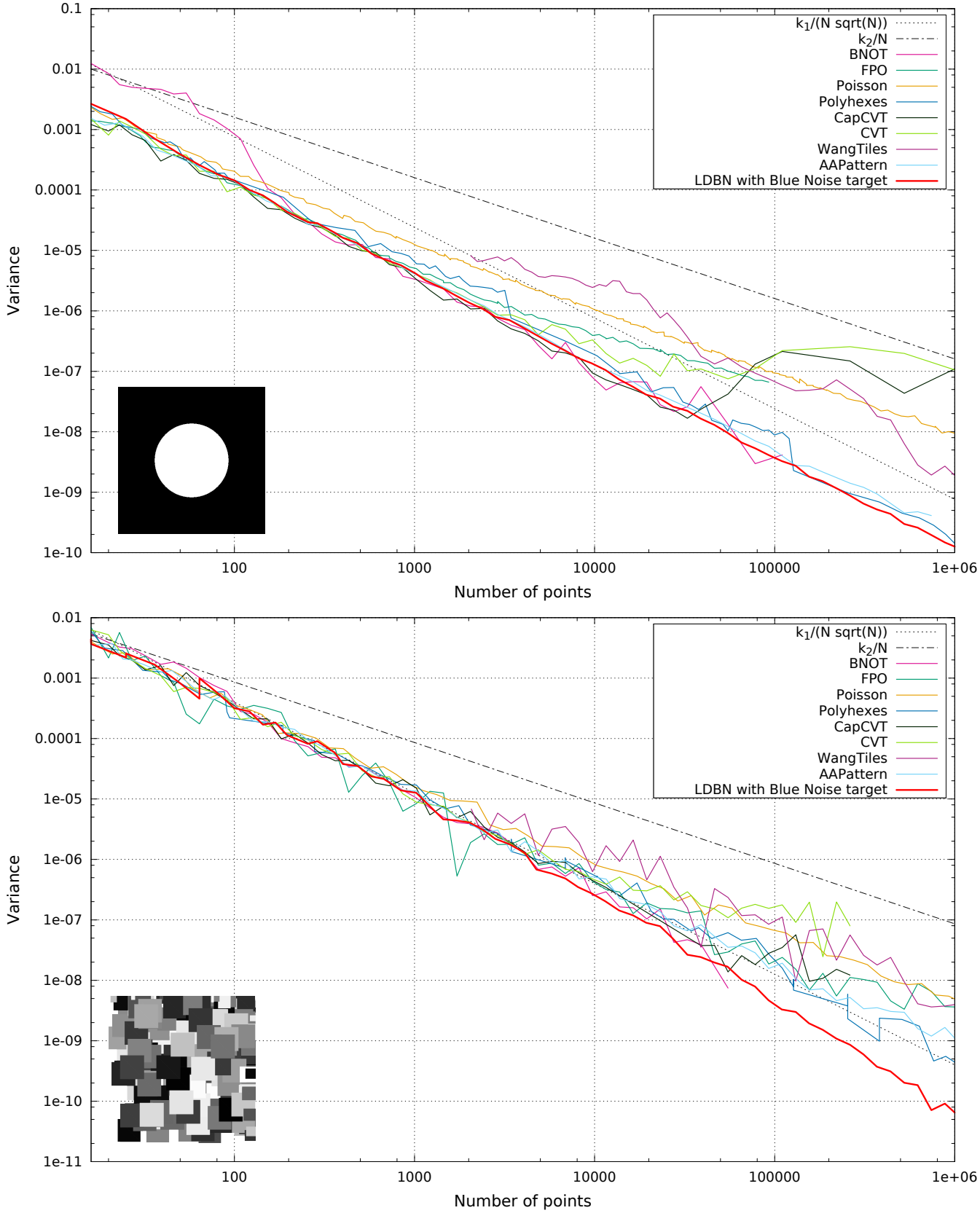

Figure 6: *Variance while integrating over an analytical disk and analytical random boxes arrangements. Comparison between our sampler and other samplers with Blue Noise spectras.*

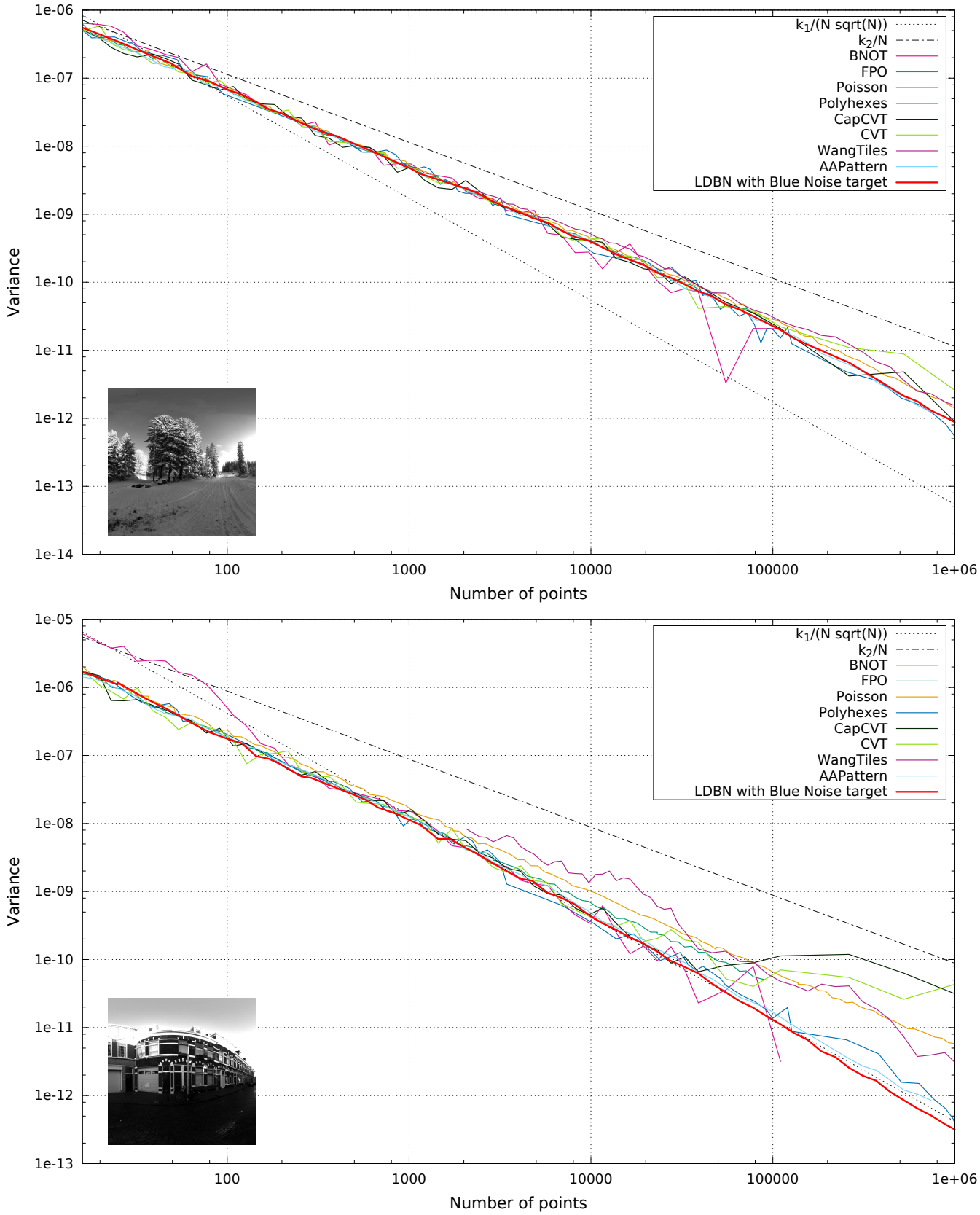

Figure 7: *Variance while integrating over two HDR Images from sIBL archive. Comparison between our sampler and other samplers with Blue Noise spectras.*

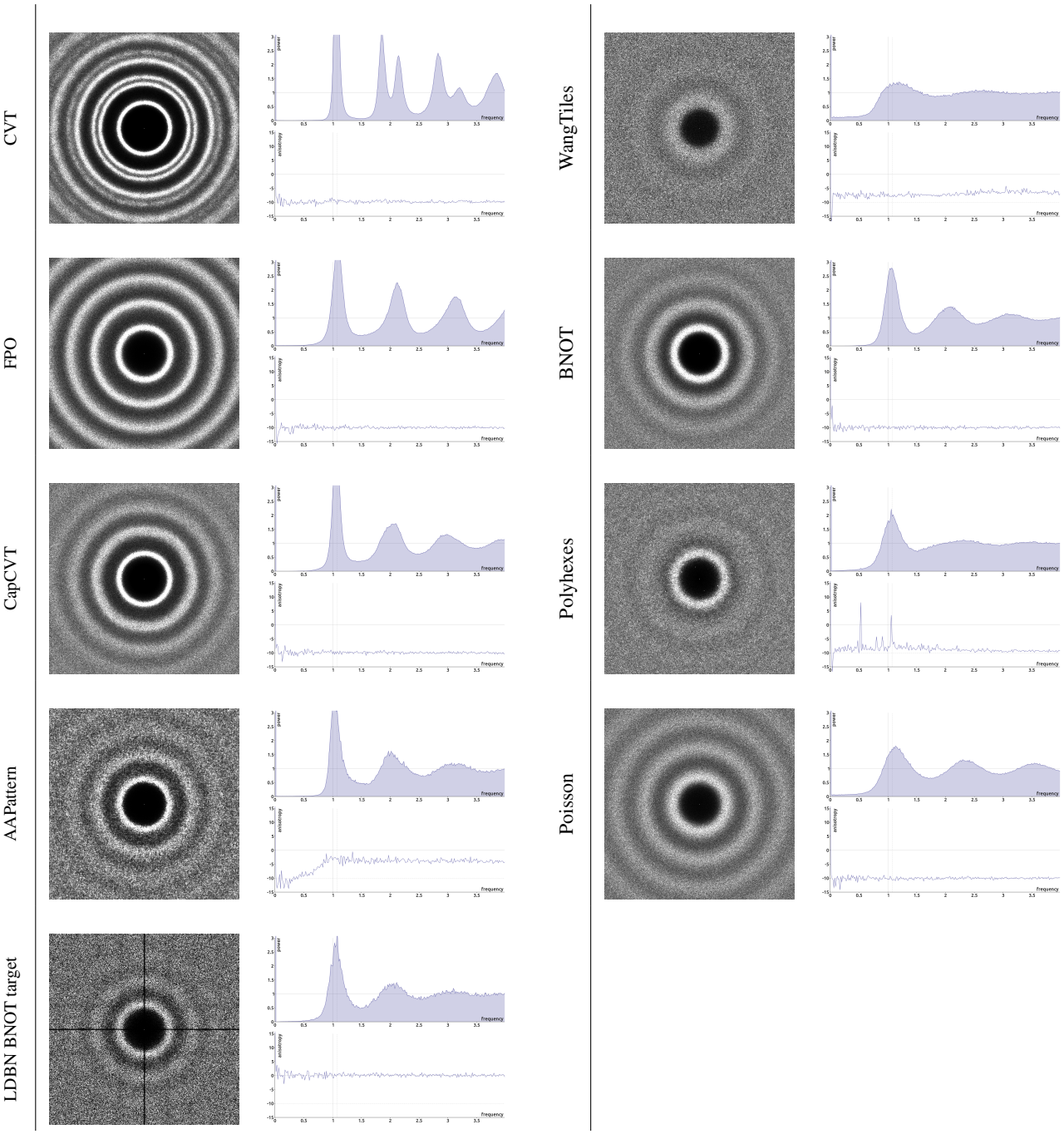

Figure 8: *Spectral results for samplers with a Blue Noise spectrum. These results were measured by averaging the spectra of 10 realizations of 4096 points. Please zoom in Fourier spectra to see narrow peaks. Please refer to the html bundle in the supplementary material to visualize the same results without scaling. The Fourier spectrum is shown on the left, the radial averaged spectrum is shown on the top right and the anisotropy is shown on the bottom right.*

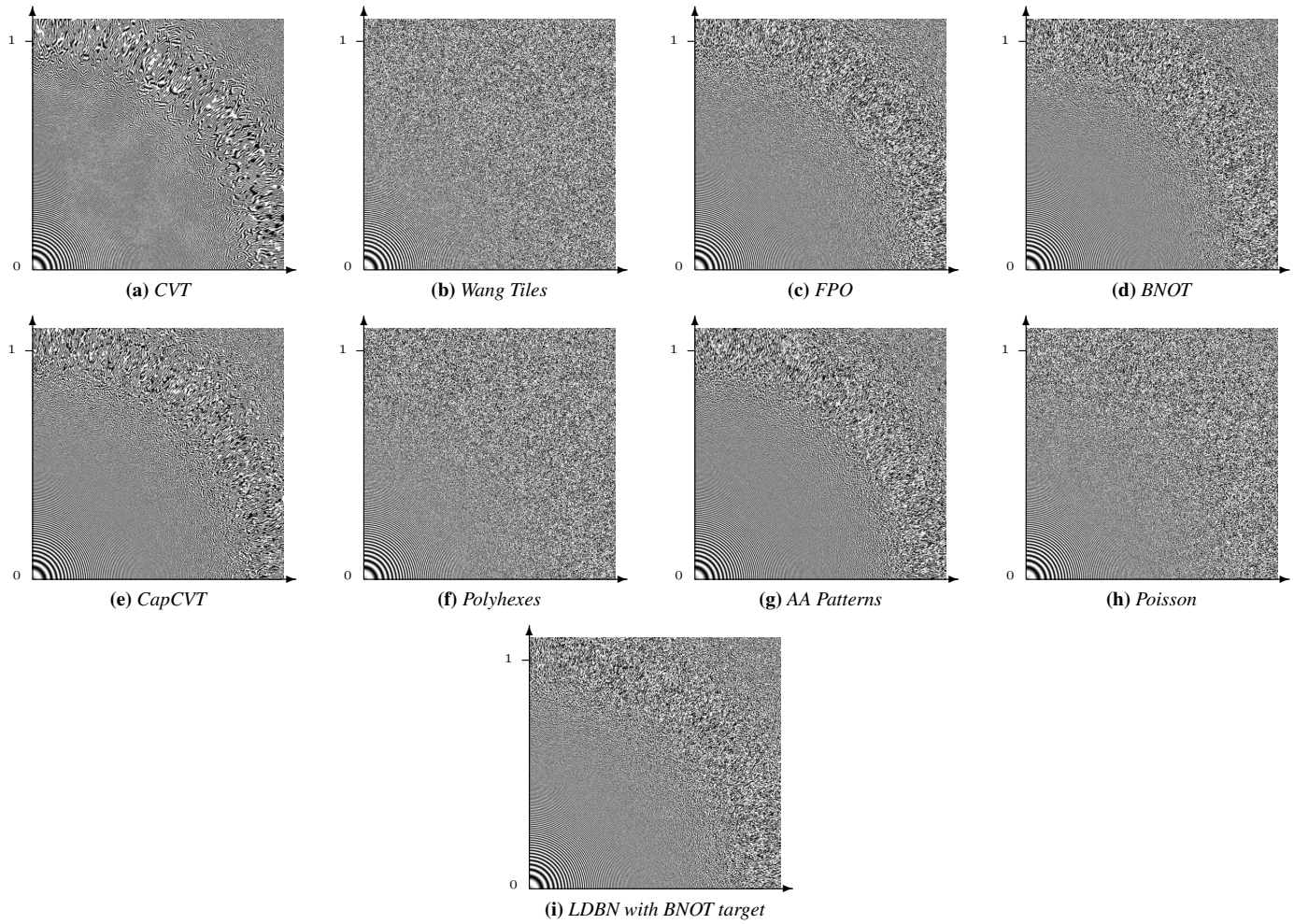

(a) *CVT* **(b)** *Wang Tiles* **(c)** *FPO* **(d)** *BNOT*

(e) *CapCVT* **(f)** *Polyhexes* **(g)** *AA Patterns* **(h)** *Poisson*

(i) *LDBN with BNOT target*

Figure 9: *Result of the zoneplate aliasing test $sin(x^2 + y^2)$ on a domain $[0, 1)$, using 1 sample per pixel and a Mitchell reconstruction filter [Mitchell and Netravali 1988]. If you can't see those results due to a filtering or scaling from your pdf viewer, you may find included with this submission a html bundle presenting the same results without scaling or filtering. The samples where generated with methods aiming at a Blue Noise Spectra*

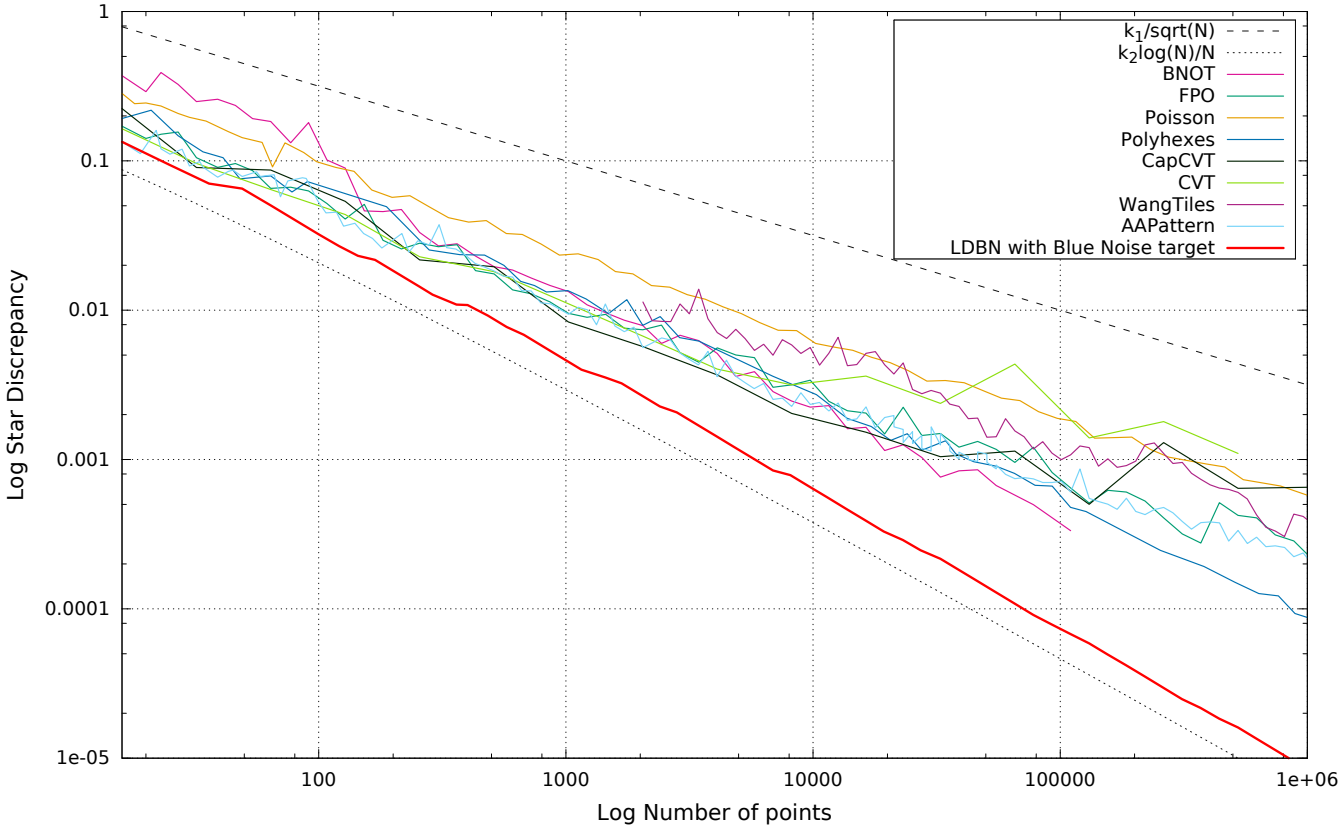

Figure 10: *Discrepancy of samplers with Blue Noise Spectra*

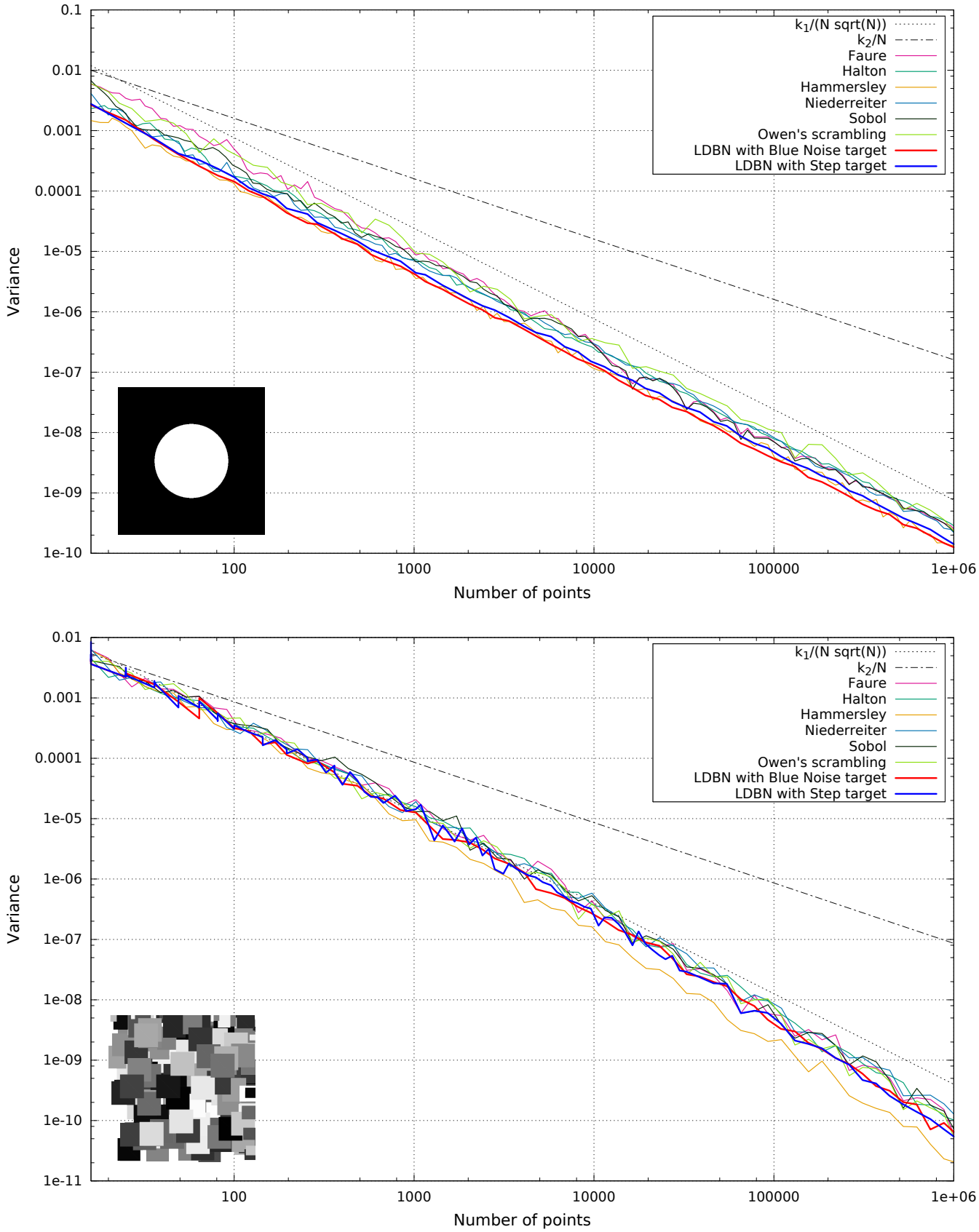

Figure 11: *Variance while integrating over an analytical disk and analytical arrangements of random boxes. Comparison between our sampler and other samplers with low discrepancy.*

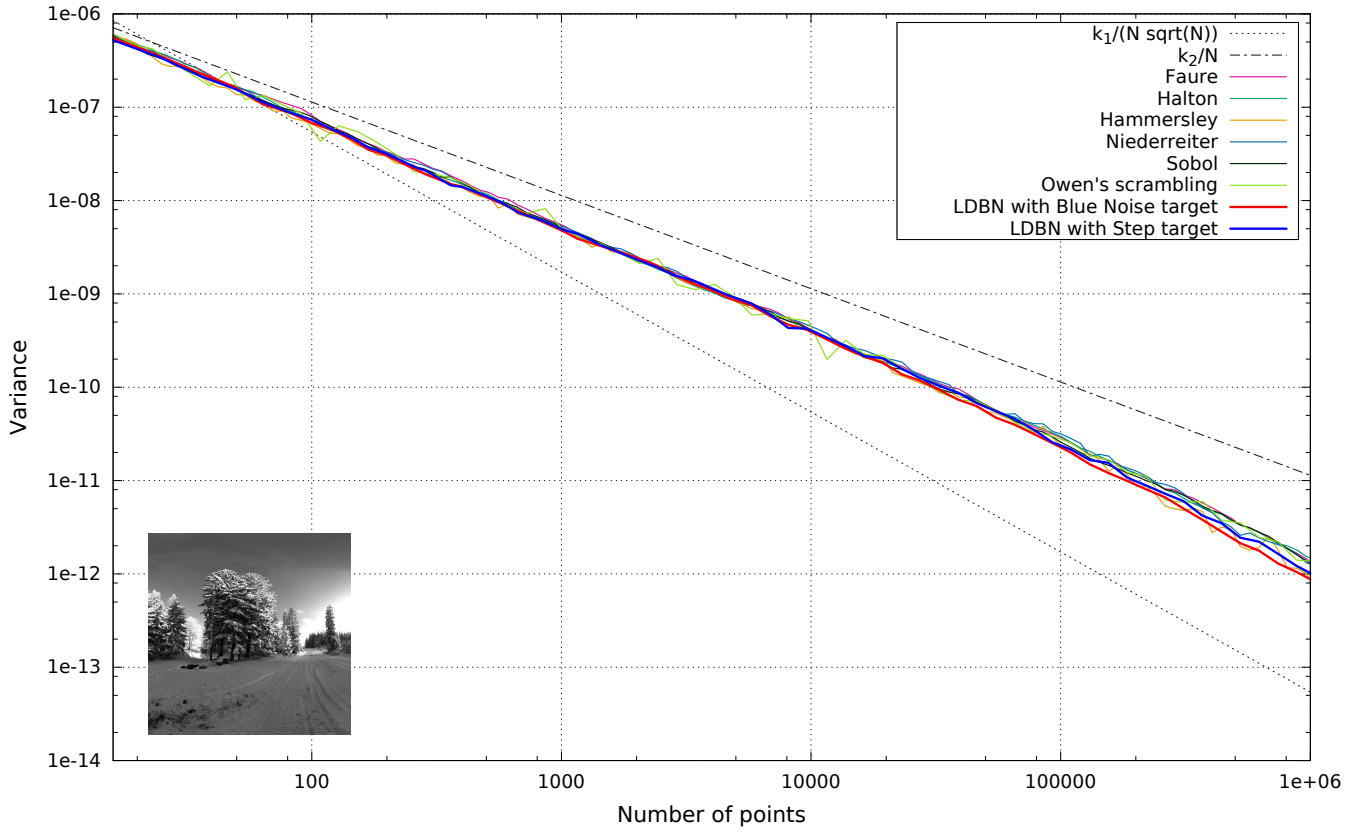

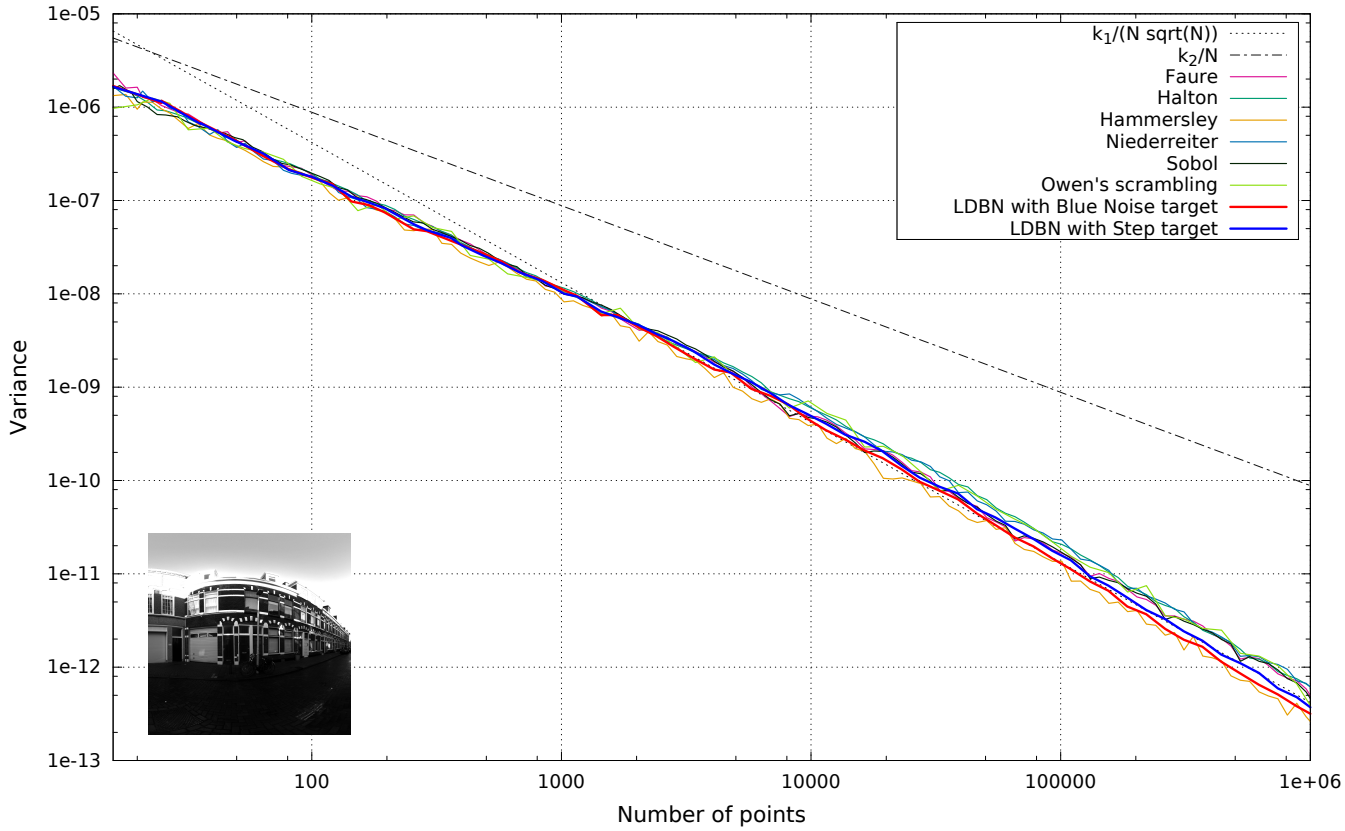

Figure 12: *Variance while integrating over two HDR Images from sIBL archive. Comparison between our sampler and other samplers with low discrepancy.*

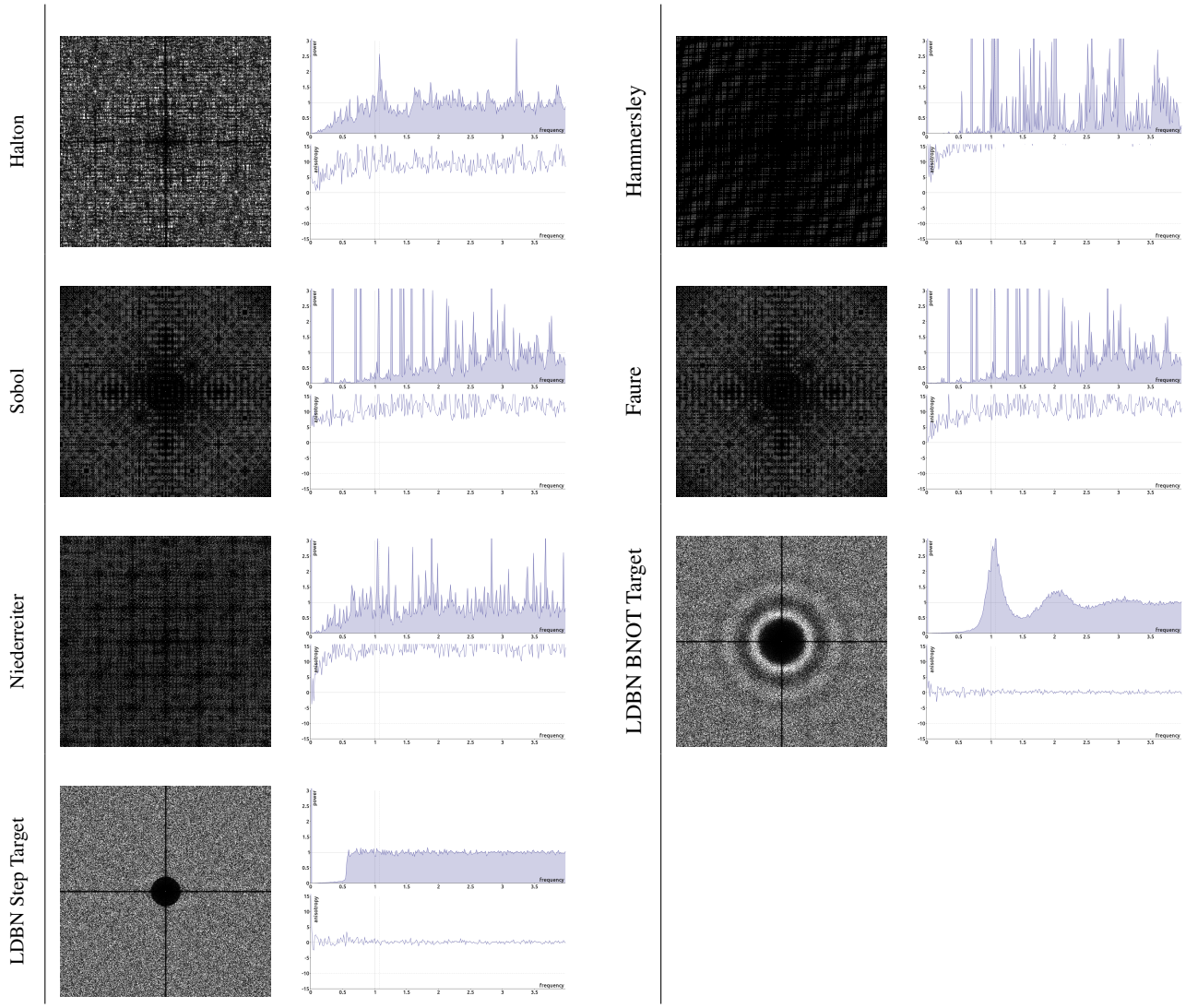

Figure 13: *Spectral results for "Low Discrepancy" samplers. These results were measured on a single realization of 4096 points. The Fourier spectrum is shown on the left, the radial averaged spectrum is shown on the top right and the anisotropy is shown on the bottom right. Please zoom in Fourier spectra to see narrow peaks. Please refer to the html bundle in the supplementary material to visualize the same results without scaling.*

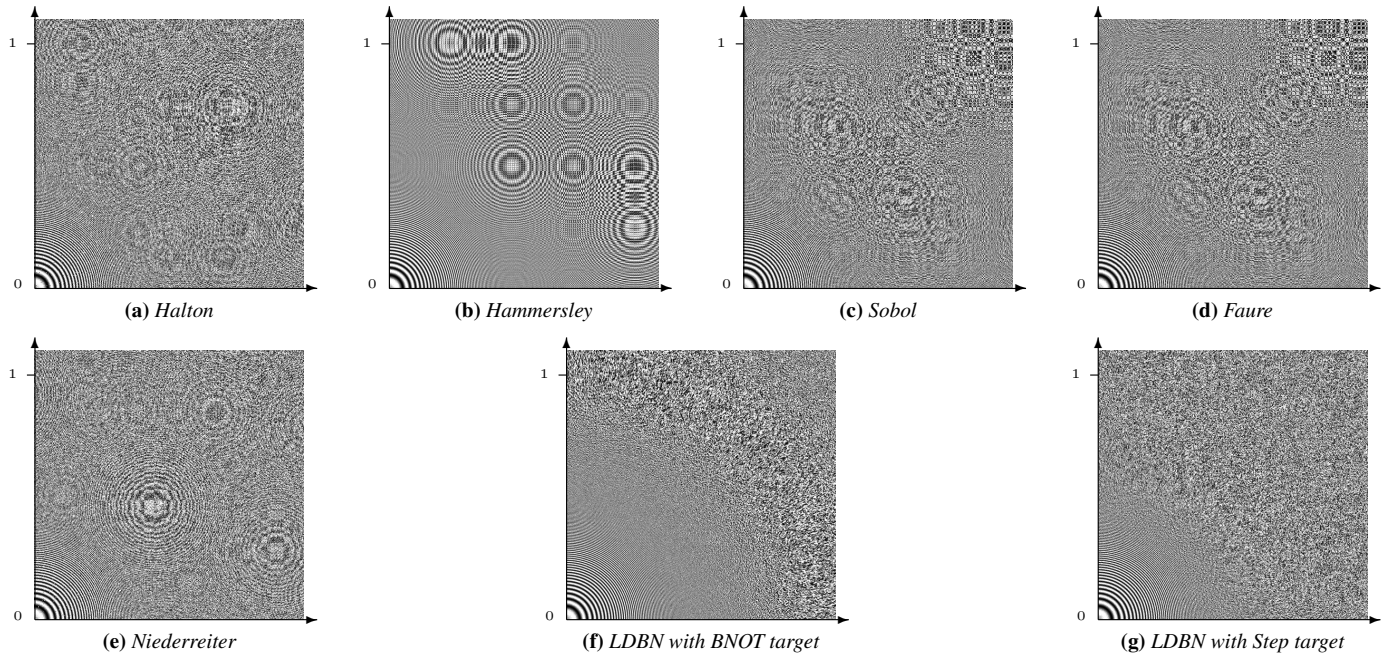

(a) *Halton* **(b)** *Hammersley* **(c)** *Sobol* **(d)** *Faure*

(e) *Niederreiter* **(f)** *LDBN with BNOT target* **(g)** *LDBN with Step target*

Figure 14: *Result of the zoneplate aliasing test $sin(x^2 + y^2)$ on a domain $[0, 1)$, using 1 sample per pixel and a Mitchell reconstruction filter [Mitchell and Netravali 1988]. If you can't see those results due to a filtering or scaling from your pdf viewer, you may find included with this submission a html bundle presenting the same results without scaling or filtering. The samples were generated with methods with Low Discrepancy*

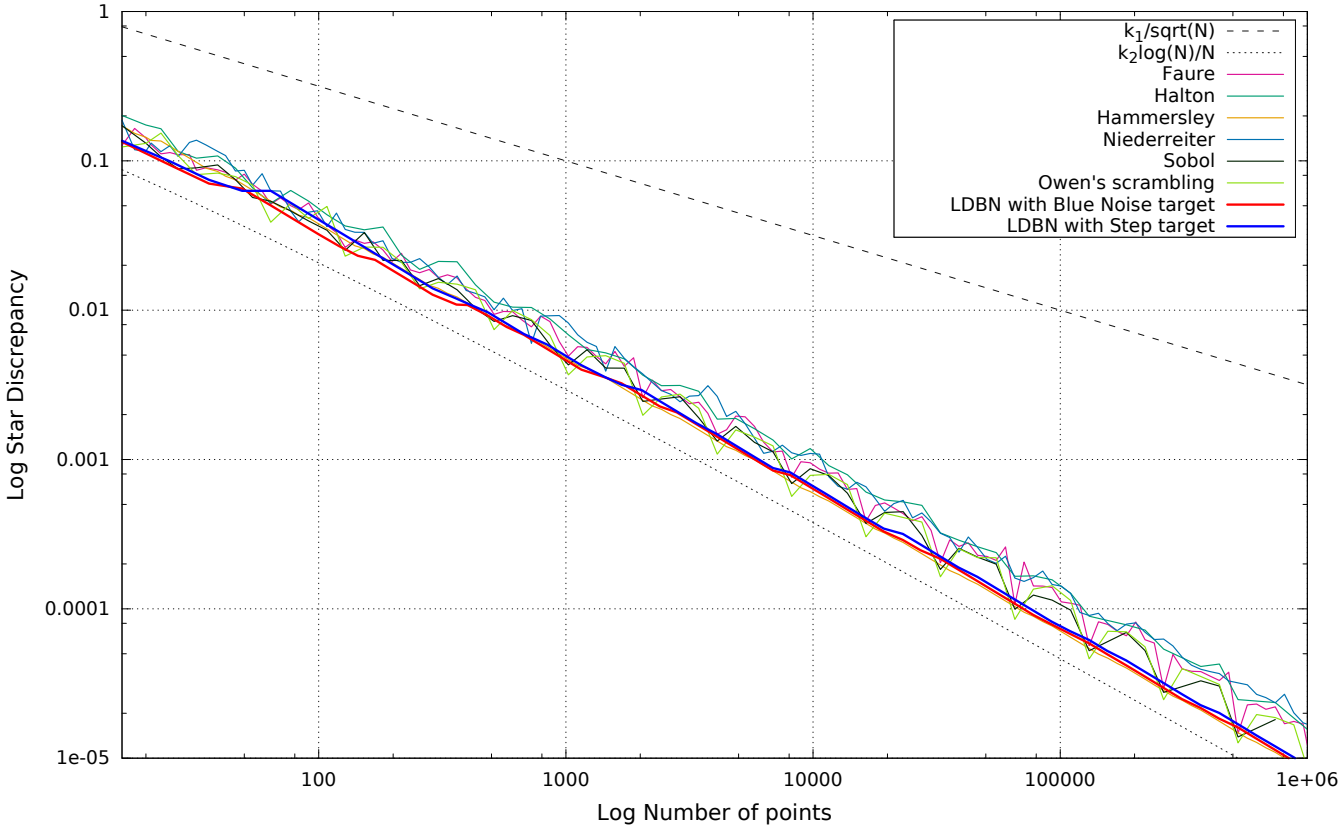

Figure 15: *Discrepancy of samplers with Low Discrepancy*

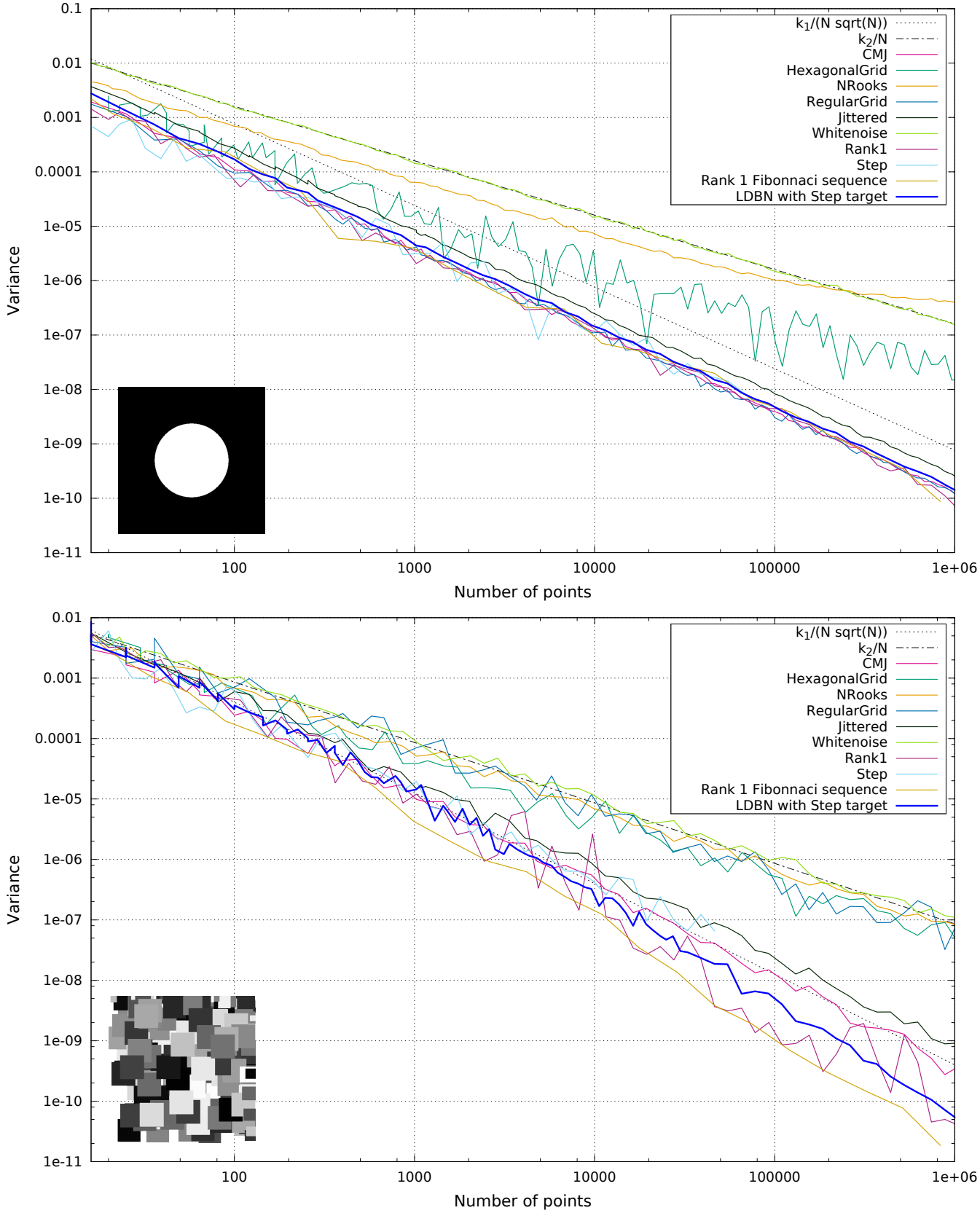

Figure 16: *Variance while integrating over an analytical disk and analytical arrangements of random boxes. Comparison between our sampler and other samplers .*

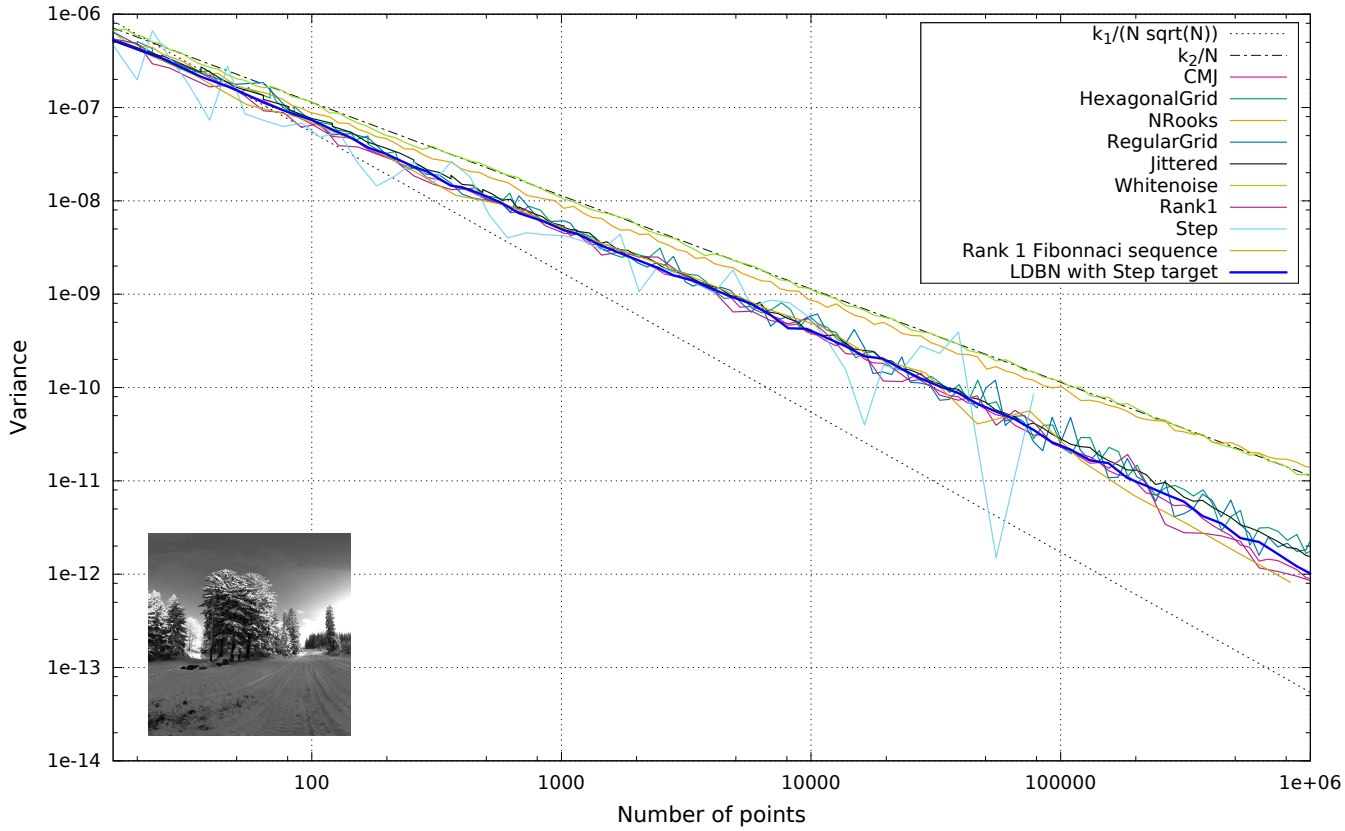

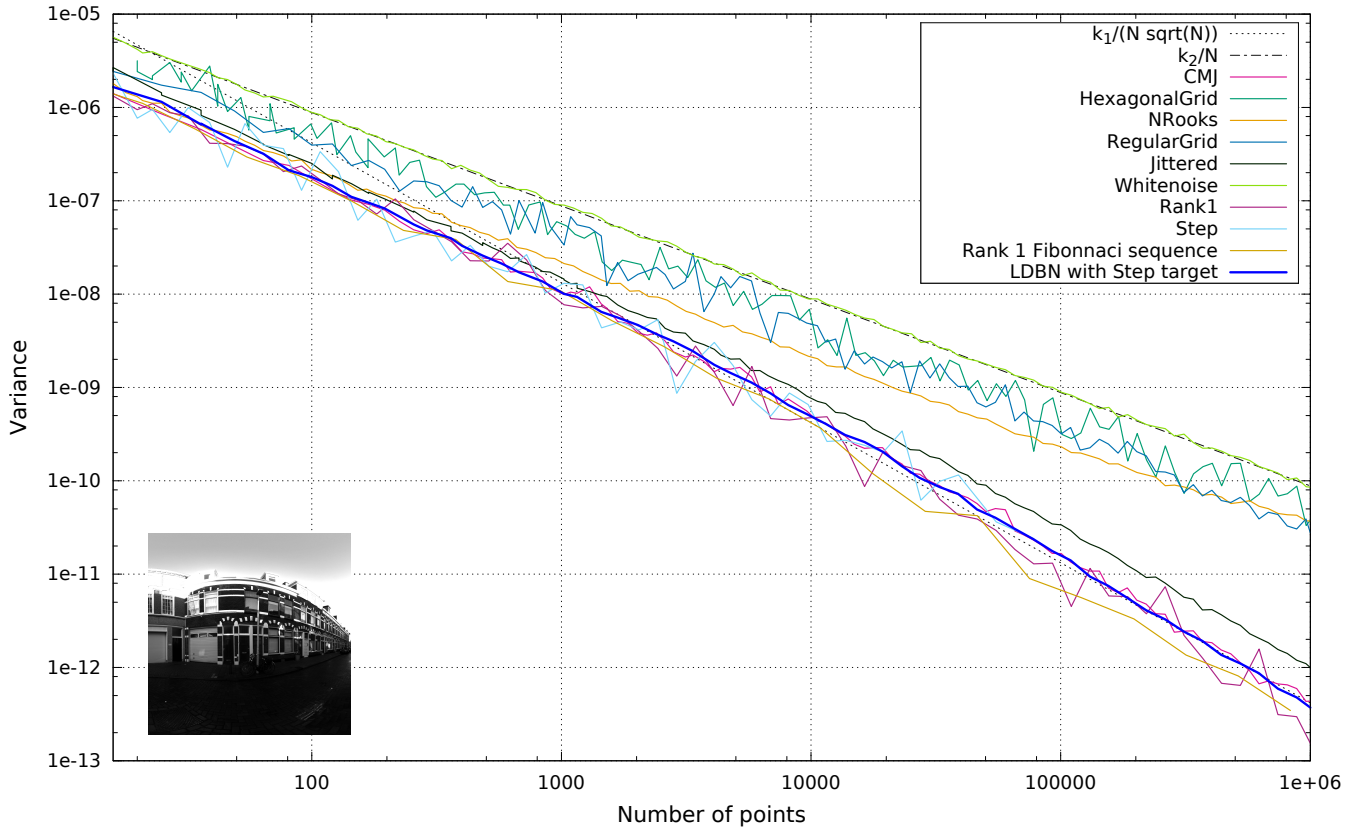

Figure 17: *Variance while integrating over two HDR Images from sIBL archive. Comparison between our sampler and other samplers.*

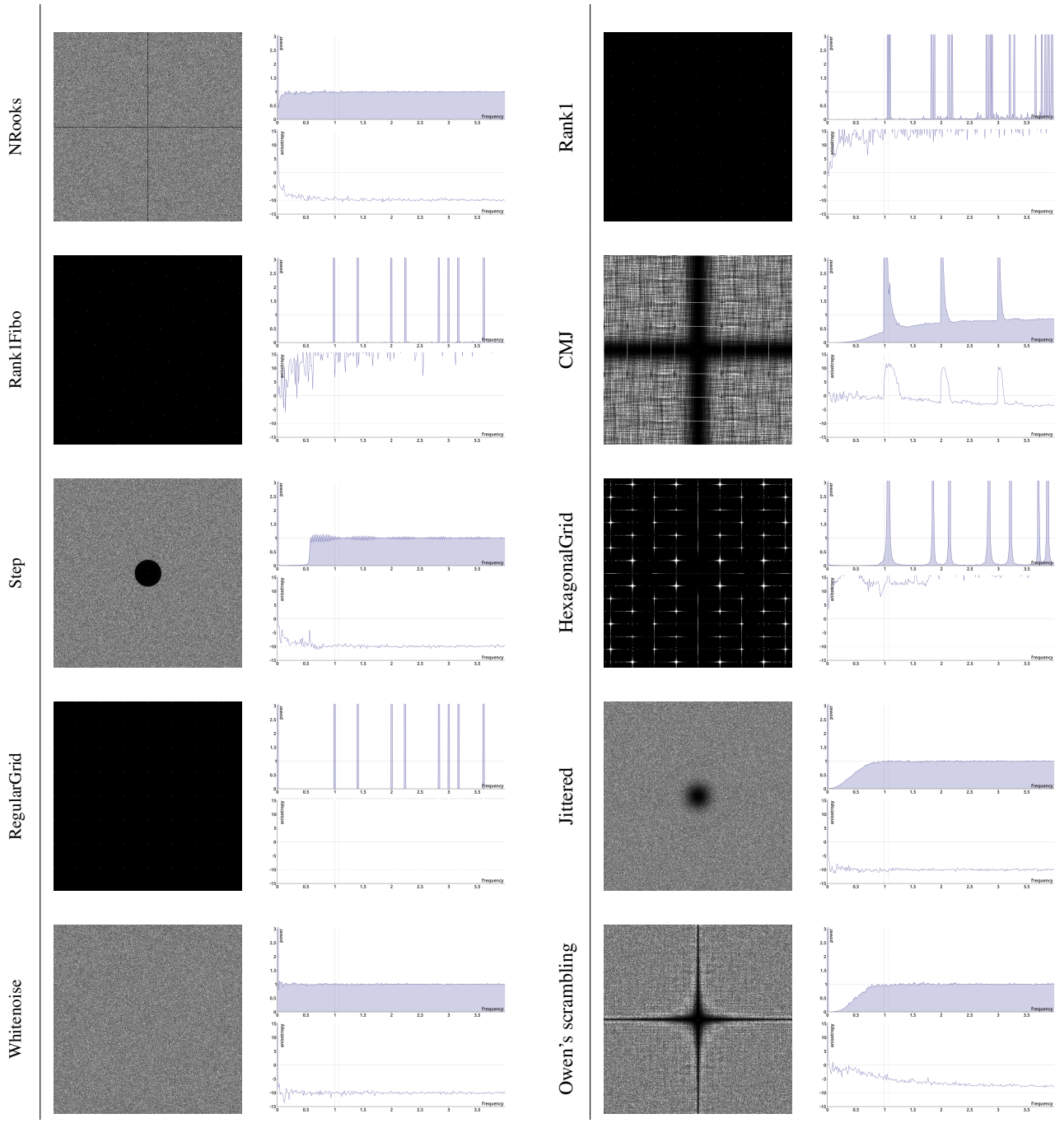

Figure 18: *Spectral results for various samplers. These results were measured on a single realisation of 4096 points for deterministic samplers, and by averaging the spectra of 10 realizations for stochastic samplers. Please zoom in Fourier spectra to see narrow peaks. Please refer to the html bundle in the supplementary material to visualize the same results without scaling. The Fourier spectrum is shown on the left, the radial averaged spectrum is shown on the top right and the anisotropy is shown on the bottom right.*

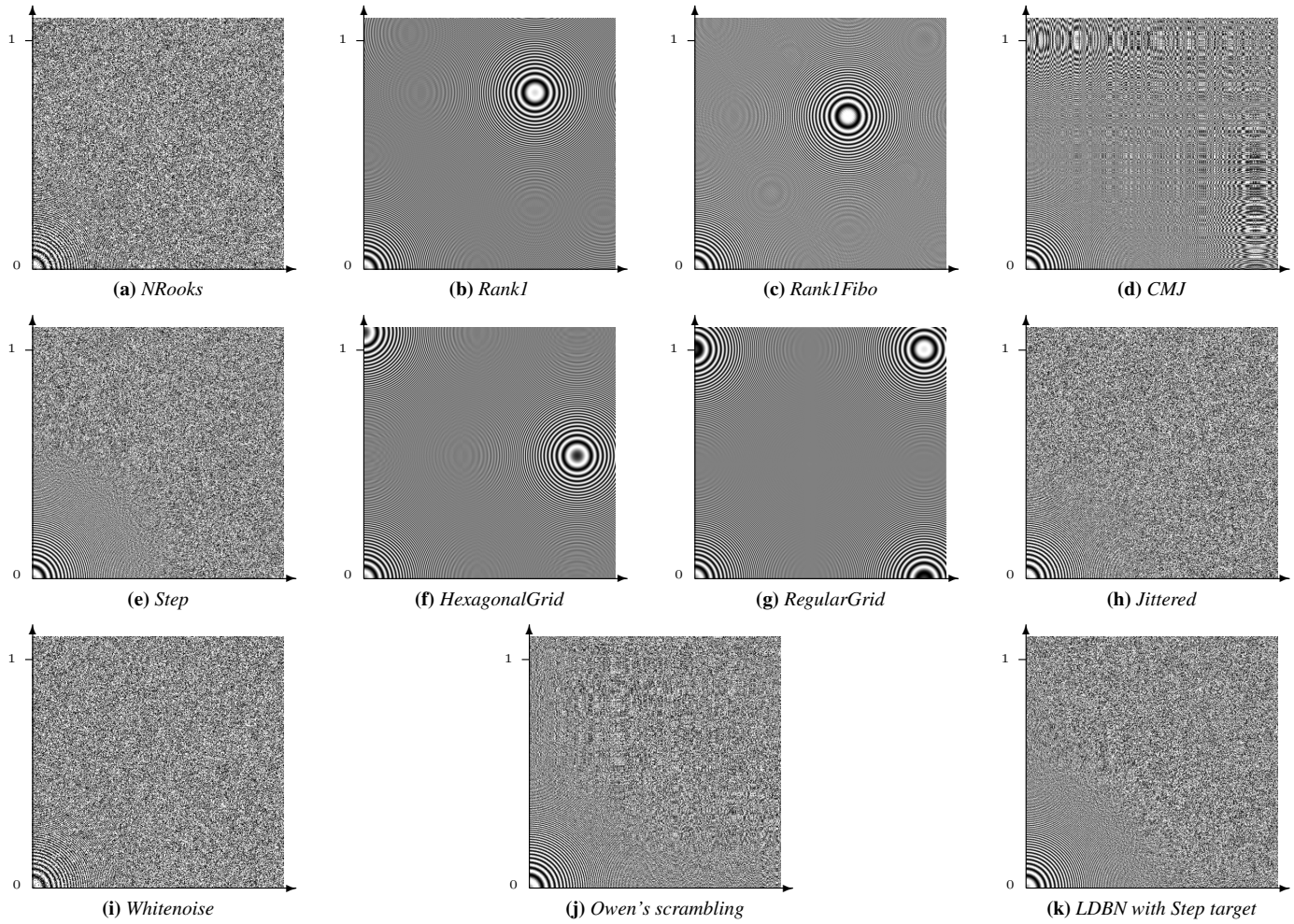

(a) *NRooks* **(b)** *Rank1* **(c)** *Rank1Fibo* **(d)** *CMJ*

(e) *Step* **(f)** *HexagonalGrid* **(g)** *RegularGrid* **(h)** *Jittered*

(i) *Whitenoise* **(j)** *Owen's scrambling* **(k)** *LDBN with Step target*

Figure 19: *Result of the zoneplate aliasing test $sin(x^2 + y^2)$ on a domain $[0, 1)$, using 1 sample per pixel and a Mitchell reconstruction filter [Mitchell and Netravali 1988]. If you can't see those results due to a filtering or scaling from your pdf viewer, you may find included with this submission a html bundle presenting the same results without scaling or filtering. The samples were generated with various methods*

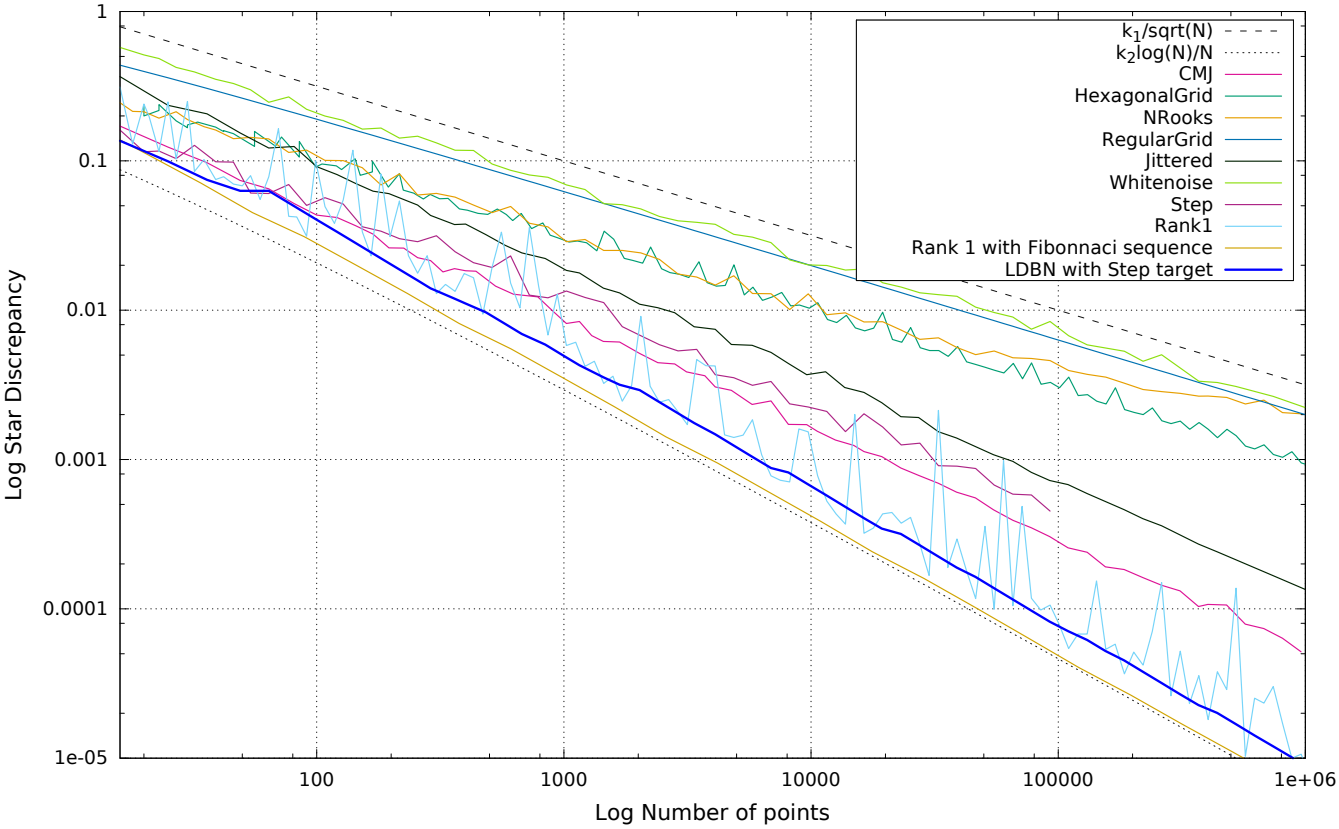

Figure 20: *Discrepancy of various sampler*